ISSN 1392 - 1207. MECHANIKA. 2011. 17(3): 264-270

Performance optimization of aluminium (U) type vibration based electromechanical Coriolis mass flow sensor using response surface methodology

Pravin P. Patil*, Satish C. Sharma, Roshan Mishra*****
**Department of Mechanical Engineering, Graphic Era University, Dehradun, Uttarakhand, India, E-mail: pravinppatil2004@gmail.com*
***Department of Mechanical and Industrial Engineering, Indian Institute of Technology Roorkee, Roorkee, Dist. Haridwar, Uttarakhand-247667, India, E-mail: sshmedme@iitr.ernet.in*
****BHEL, Hydrabad, India, E-mail: roshangreat1@gmail.com*

crossref http://dx.doi.org/10.5755/j01.mech.17.3.501

1. Introduction

The electromechanical Coriolis mass flow sensor has a tube through which a fluid to be measured flows is supported at one end or both ends thereof , and vibration is applied to a portion of the tube around the supporting point in a direction vertical to the flowing direction of the tube. The Coriolis mass flow sensor utilizes the fact that the Coriolis forces applied is referred to the flow tube when vibration is thus applied thereto are proportional to a mass flow rate [1]. Successful operating performance of mass flow sensor depends on the selection of suitable design variables and conditions [2]. Therefore it is important to determine the operating design parameters at which the response reaches its optimum. The optimum could be either a maximum or a minimum of a function of the design parameters. One of the methodologies for obtaining the optimum results is response surface methodology (RSM). Performance optimization requires many tests. However, the total number of experiments required can be reduced depending on the experimental design technique. It is essential that an experimental design methodology is very economical for extracting the maximum amount of complex information while saving significant experimental time, material used for analyses and personnel costs [3].

This methodology is actually a combination of statistical and mathematical techniques and it was primarily proposed by Box and Wilson [4] to optimize operating conditions in the chemical industry. RSM has been further developed and improved during the past decades with applications in many scientific realms. Myers et al [5, 6] present reviews of RSM in its basic development period and a comparison of different RS metamodels with different applications is given by Rutherford et al [7]. A comprehensive description of RSM theory can be found in [3]. Apart from chemistry and other realms of industry, RSM has also been introduced into the reliability analysis and model validation of mechanical and civil structures [8, 9]. This methodology has been widely employed in many applications such as design optimization, response prediction and model validation. But so far the literature related to its application in Coriolis mass flow sensing is scarce.

Thus, the primary objectives of this study was therefore to use RSM in conjunction with central composite design, which requires fewer tests than a full factorial design to establish the functional relationships between three operating variables namely sensor location, drive frequency and mass flow rate, and phase shift for optimum performance of Coriolis mass flow sensor. These relationships can then be used to determine the optimal operating parameters. In the following sections, the application of RSM and CCD to modeling and optimization of the influence of three operating design variables on the performance of Coriolis mass flow sensor is discussed.

2. Response surface methodology (RSM)

RSM is a collection of statistical and mathematical methods that are useful for modeling and analyzing engineering problems. In this technique, the main objective is to optimize the response surface that is influenced by various process parameters. RSM also quantifies the relationship between the controllable input parameters and the obtained response surfaces [3].

The design procedure for RSM is as follows:
1. Performing a series of experiments for adequate and reliable measurement of the response of interest. 2. Developing a mathematical model of the second-order response surface with the best fit. 3. Determining the optimal set of experimental parameters that produce a maximum or minimum value of response. 4. Representing the direct and interactive effects of process parameters through two and three-dimensional (3D) plots.

If all variables are assumed to be measurable, the response surface can be expressed as follows

$$y = f(x_1, x_2, ..., x_i) \quad (1)$$

where y is the answer of the system, and x_i the variables of action called factors.

The goal is to optimize the response variable y. An important assumption is that the independent variables are continuous and controllable by experiments with negligible errors. The task then is to find a suitable approximation for the true functional relationship between independent variables and the response surface [3].

3. Central composite design (CCD)

As mentioned above, the first requirement for RSM involves the design of experiments to achieve adequate and reliable measurement of the response of interest. To meet this requirement, an appropriate experimental

design technique has to be employed. The experimental design techniques commonly used for process analysis and modeling are the full factorial, partial factorial and central composite designs. A full factorial design requires at least three levels per variable to estimate the coefficients of the quadratic terms in the response model [4]. A partial factorial design requires fewer experiments than the full factorial design. However, the former is particularly useful if certain variables are already known to show no interaction [10]. An effective alternative to factorial design is central composite design (CCD), originally developed by Box and Wilson [4] and improved upon by Box and Hunter [11]. CCD gives almost as much information as a three-level factorial, requires many fewer tests than the full factorial design and has been shown to be sufficient to describe the majority of steady-state process responses. Hence in this study, it was decided to use CCD to design the experiments. The number of tests required for CCD includes the standard 2k factorial with its origin at the center, 2k points fixed axially at a distance, say β, from the center to generate the quadratic terms, and replicate tests at the center; where k is the number of variables. The axial points are chosen such that they allow rotatability [11], which ensures that the variance of the model prediction is constant at all points equidistant from the design center. Replicates of the test at the center are very important as they provide an independent estimate of the experimental error. For three variables, the recommended number of tests at the center is six [11]. Hence the total number of tests required for the three independent variables is 2^3+ (2×3) + 6 = 20. Once the desired ranges of values of the variables are defined, they are coded to lie at ±1 for the factorial points, 0 for the center points and ±β for the axial points [11]. The codes are calculated as functions of the range of interest of each factor as shown in Table 1. When the response data are obtained from the test work, a regression analysis is carried out to determine the coefficients of the response model (b_1, b_2, …, b_n), their standard errors and significance. In addition to the constant (b_0) and error (ε) terms, the response model incorporates [10]:

- linear terms in each of the variables $(x_1, x_2, ..., x_n)$;
- squared terms in each of the variables $(x_1^2, x_2^2, ..., x_n^2)$;
- first order interaction terms for each paired combination $(x_1, x_2, x_1x_3, ..., x_{n-i}x_n)$.

Thus for the three variables under consideration, the response model is

$$y = (b_o + \varepsilon) + \sum_{i=1}^{3} b_i x_i + \sum_{i=1}^{3} b_i x_i^2 + \sum_{i=1}^{3} \sum_{j=i+1}^{3} b_{ij} x_i x_j \qquad (2)$$

The b coefficients are obtained by the least squares method.

In general Eq. (2) can be written in matrix form

$$Y = bX + \varepsilon \qquad (3)$$

where Y is defined to be a matrix of measured values and X to be a matrix of independent variables. The matrices b and ε consist of coefficients and errors, respectively. The solution of Eq. (3) can be obtained by the matrix approach [3]

$$b = (X' \bullet X)^{-1} X' \bullet Y \qquad (4)$$

where X' is the transpose of the matrix X and $(X' \bullet X)^{-1}$ is the inverse of the matrix $X' \bullet X$.

The coefficients, i.e. the main effect (b_i) and two-factor interactions (b_{ij}) can be estimated from the experimental results by computer simulation programming applying the method of least squares using the mathematical software package design expert [12].

4. Experimental design

CCD was used to design the experiments to the reason mentioned above. In order to obtain the required data, the range of values of each of the three variables was defined as follows: sensor location of 60 - 120 mm, drive frequency of 62 - 64 Hz, and mass flow rate of 0.1 - 0.3 kg/s. Applying the relationships in Table 1, the values of the codes were calculated as shown in Table 2. These were then used to determine the actual levels of the variables for each of the 20 experiments (Table 3).

Table 1

Relationship between coded and actual values of a variable [3]

Code	Actual value of variable
$-\beta$	x_{min}
−1	$[(x_{max}+x_{min})/2]-[(x_{max}-x_{min})/2\alpha]$
0	$(x_{max}+x_{min})/2$
+1	$[(x_{max}+x_{min})/2]+[(x_{max}-x_{min})/2\alpha]$
$+\beta$	x_{min}

5. Experimental setup and procedure

Trials were conducted in an indigenously deve–loped setup based on the Coriolis technology for vibration based aluminium U tube CMFS. A brief description of the set-up and the Coriolis action is presented as follows. The Experimental set up used in the present study has been designed on Pro Engineer Wildfire modelling software and later manufactured at the Instrumentation laboratory of Mechanical and Industrial Engineering Department, IIT, Roorkee.

Table 2

Independent variables and their levels for CCD

Design parameter	Symbol	unit	-1	0	+1
			Low	center	high
Mass flow rate	X_1	Kg/s	0.1	0.2	0.3
Sensor location (SL)	X_2	mm	60	90	120
Drive frequency (DF)	X_3	Hz	62	63	64

The actual photograph of the experimental setup has been shown in Fig. 1, which consists of the several functional elements such as: Hydraulic bench for providing regulated water supply to the flowmeter. Test bench for

supporting the tubes of the Coriolis mass flow sensor. Excitation system for providing mechanical excitation to the Coriolis mass flow sensor, consists of an electrodynamics shaker, control unit, accelerometer and vibration sensor. Virtual instrumentation comprising of noncontact optical sensors, and a signal conditioning unit as shown in Fig. 1. A Coriolis mass flow sensor measures mass flow directly, which is based on the conservation of angular momentum, as it applies to the Coriolis acceleration of a given fluid.

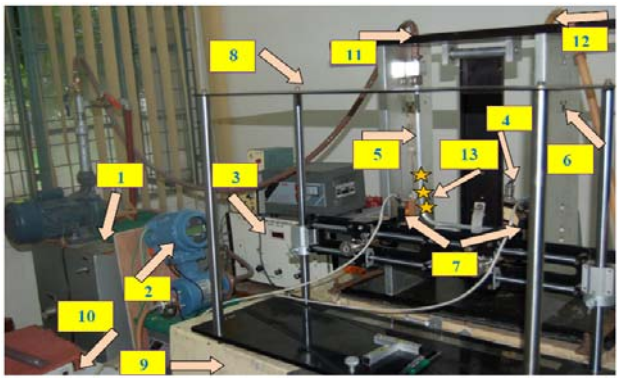

Fig. 1 Actual photographic view of experimental setup. Various design components as follows: *1* - hydraulic bench, *2* - electromagnetic flowmeter, *3* - vibration control unit, *4* - vibration driver,*5* - U tube, *6* - test bench, *7* - laser sensors, *8* - sensor holding stand, *9* - foundation, *10* - data acquisition box, *11* - inlet pipe, *12* - outlet pipe, *13* - sensor locations

In principle, as shown in Fig. 2**,** a Coriolis mass flow sensor consists of a tube with a fixed inlet and outlet, which is vibrated about the axis, formed by the inlet and outlet ends. The tube used in this study is Aluminium U shaped vibrating tube, and is made to vibrate using an electrodynamics vibration shaker attached at point as shown in figure. Optical analog displacement sensors are mounted as indicated in figure and is labeled as SL on two limbs of tube to measure displacement signals from the vibrating tube. This means that liquid flow is measured by transferring vibrational energy from the meter tubing to the flowing liquid and back to the meter. To appreciate this princepple, imagine a vibrating tube shown in Fig. 2. If no liquid is flowing, the excitation in the middle of the tube will

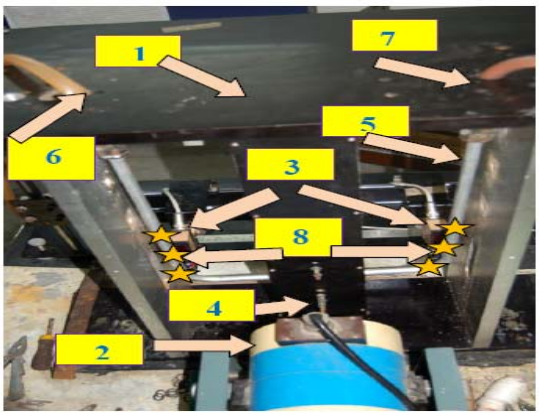

Fig. 2 Vibrating aluminium U type tube: *1* - test bench, *2* - vibration driver, *3* - laser sensors, *4* - vibration driver rod, *5* - U tube, *6* - inlet pipe, *7* - outlet pipe, *8* - sensor locations

cause both arms to vibrate in phase. Mass flowing into the tube starts to receive vibrational energy from the tube walls as it enters the first bend. In this process, the tube loses the same amount of energy. The result is that the phase of the vibrational cycle lags at sensor location of one limbs, the reverse will happen at the location of another limbs. The liquid is vibrating as it enters the bend, but transfers this energy to the pipe. The result is that the mass flow advances the vibrational phase at the sensor location of another limb. When combined, these two changes in vibrational phase produce a twisting of the flow tube. The amplitude of this twist is directly proportional to the mass flow rate and is nearly independent of the temperature, density, or viscosity of the liquid involved.

The details of the experimental procedure used to conduct the present study have been described in Fig. 3 as shown below. The hydraulic unit for providing regulated

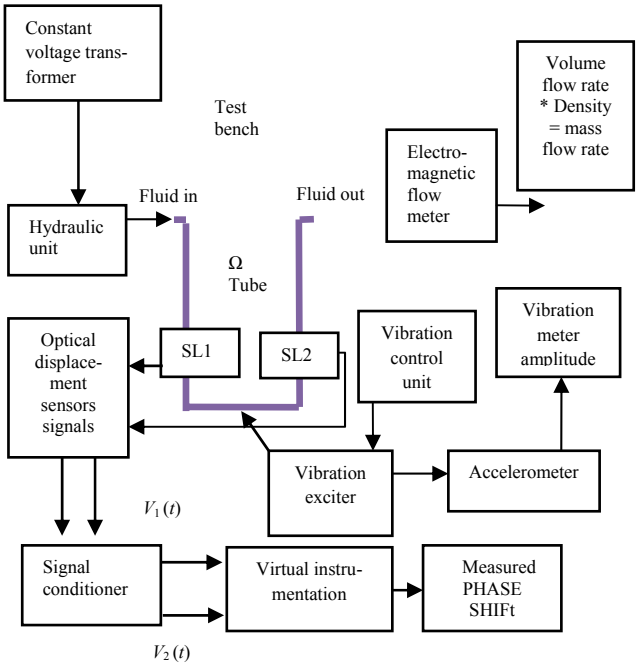

Fig. 3 Flow diagram showing experimental procedure

water supply to the mass flow sensor. The hydraulic unit derives its power from the constant voltage transformer (CVT) to maintain constant flow rate. The U-tube is made to vibrate using an electronic shaker. An accelerometer is attached to the shaker which measures the velocity, amplitude and acceleration of the vibration induced by the electronic shaker. The accelerometer gives the feedback to the vibration meter which is observed for maintaining the constant amplitude. A pair of optical displacement sensors has been placed on the mechanical positioning attachment facing the two limbs of the U-tube. The output terminals of the sensors have been connected to the input of the NI-DAQ through a signal conditioner. The processing of the signals is processed in Labview to extract phase shift from the two acquired signals using FFT. Accuracy and repeatability for each experiment was achieved with the same input conditions until stabilized output was achieved.

6. Model development and results

Results from the experiments are summarized in Table 3. Considering the effects of main factors and the

interactions between two factors, Eq. (2) takes the form

$$y = \beta_0 + \beta_1 x_1 + \beta_2 x_2 + \beta_3 x_3 + \beta_{11} x_1^2 + \beta_{22} x_2^2 + \\ + \beta_{33} x_3^2 + \beta_{12} x_1 x_2 + \beta_{13} x_1 x_3 + \beta_{23} x_2 x_3 \quad (5)$$

The coefficients, i.e. the main effect (β_i) and two-factor interactions (β_{ij}) were estimated from the experimental results using a computer simulation applying the method of least squares in design expert simulation software. From the experimental results in Table 3 and Eq. (4), the second-order response functions representing phase shift can be expressed as a function of the three operating parameters of CMFS, namely the sensor location, drive frequency, mass flow rate.

Table 3
Central composite design consisting of experiments for the study of three experimental factors in coded and actual levels with experimental results

Test run	Coded level of variables			Actual level of variables			Observed phase shift
	X_1	X_2	X_3	Sensor location	Drive frequency	Mass flow rate	
				mm	Hz	kg/s	degrees
1	1	-1	-1	120	62	0.1	1.542886
2	-1	1	-1	60	64	0.1	1.238847
3	0	0	0	90	63	0.2	4.01569
4	0	1	0	90	64	0.2	2.420494
5	1	1	1	120	64	0.3	2.920386
6	1	-1	1	120	62	0.3	2.449727
7	0	0	0	90	63	0.2	4.618508
8	-1	0	0	60	63	0.2	2.85711
9	-1	-1	1	60	62	0.3	1.848543
10	0	0	0	90	63	0.2	4.42002
11	0	0	0	90	63	0.2	4.16356
12	0	-1	0	90	62	0.2	1.449934
13	1	0	0	120	63	0.2	4.34051
14	0	0	1	90	63	0.3	4.911829
15	0	0	0	90	63	0.2	3.90024
16	-1	-1	-1	60	62	0.1	0.835637
17	1	1	-1	120	64	0.1	1.609594
18	0	0	0	90	63	0.2	4.152364
19	0	0	-1	90	63	0.1	3.893454
20	-1	1	1	60	64	0.3	3.068856

The relationship between response (phase shift) and operating parameters were obtained for coded unit as follows:

In coded variables

$$\text{Phase shift} = 4.19 + 0.74X_1 + 0.31X_2 + 0.61X_3 - \\ -0.33X_1^2 - 1.99X_2^2 - 0.14X_1X_2 - 0.078X_1X_3 + \\ +0.15X_2X_3 - 0.55X_1X_2^2 \quad (6)$$

The response factors at any regime in the interval of our experimental design can be calculated from Eq. (6). The predicted values for phase shift with observed values are given in Table 4. The observed values and predicted values of phase shift obtained using model Eq. (6) is presented in Fig. 4 as can be seen, there is a good agreement between predicted values and the observed data points (R^2 value of 0.97 for phase shift).

Table 4
Experimental and predicted values of phase shift

Test run	Actual level of variables			Observed value of phase shift	Predicted value of phase shift
	Sensor location	Drive frequency	Mass flow rate		
	mm	Hz	kg/s	degrees	
1	120	62	0.1	1.542886	1.509698
2	60	64	0.1	1.238847	1.291726
3	90	63	0.2	4.01569	4.192984
4	90	64	0.2	2.420494	2.514256
5	120	64	0.3	2.920386	2.923913
6	120	62	0.3	2.449727	2.263899
7	90	63	0.2	4.618508	4.192984
8	60	63	0.2	2.85711	3.123008
9	60	62	0.3	1.848543	1.766002
10	90	63	0.2	4.42002	4.192984
11	90	63	0.2	4.16356	4.192984
12	90	62	0.2	1.449934	1.887966
13	120	63	0.2	4.34051	4.606408
14	90	63	0.3	4.911829	4.800876
15	90	63	0.2	3.90024	4.192984
16	60	62	0.1	0.835637	0.699161
17	120	64	0.1	1.609594	1.559185
18	90	63	0.2	4.152364	4.192984
19	90	63	0.1	3.893454	3.585092
20	60	64	0.3	3.068856	2.969095

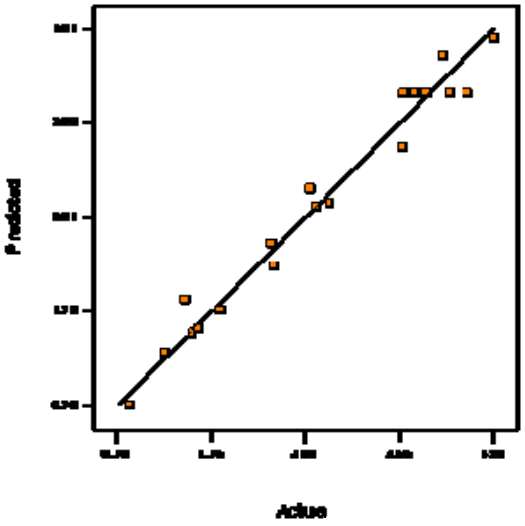

Fig. 4 Relation between experimental and predicted phase shift values using Eq. 6

6.1. Effect of variables on phase shift

In order to gain a better understanding of the results, the predicted models are presented in Fig. 5 through 7 as the 3D response surface plots. Fig. 5 shows the effect of the sensor location and the Drive frequency at the high level of mass flow rate. As can be seen, a higher phase shift can be achieved maintaining a optimum level of drive frequency and sensor location. Fig. 6 shows the effect of the mass flow rate and sensor location at the center level of Drive frequency. The general form of three-dimensional relationship is similar to the previous figure, i.e. a higher phase shift is obtained with optimum level of sensor location but maximum level of mass flow rate.

Fig. 7 shows the effect of the mass flow rate and the drive frequency at the center level of sensor location. It can be seen that a higher phase shift can be obtained with

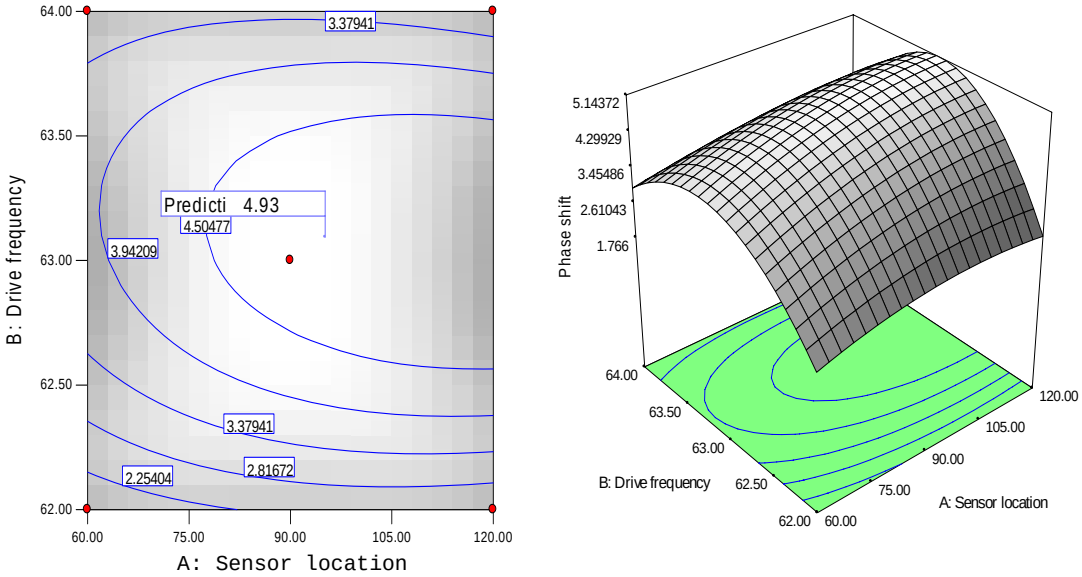

Fig. 5 Response surface predicting phase shift from the model equation: effect of the sensor location and the drive frequency at the high level of mass flow rate

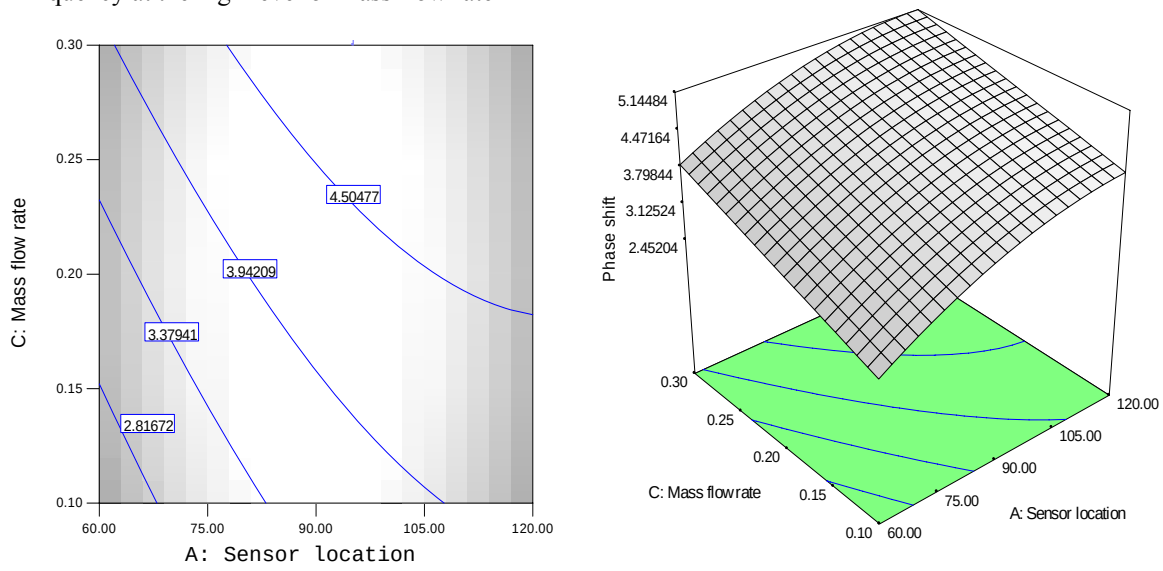

Fig. 6 Response surface predicting phase shift from the model equation: effect of the mass flow rate and sensor location at the center level of drive frequency

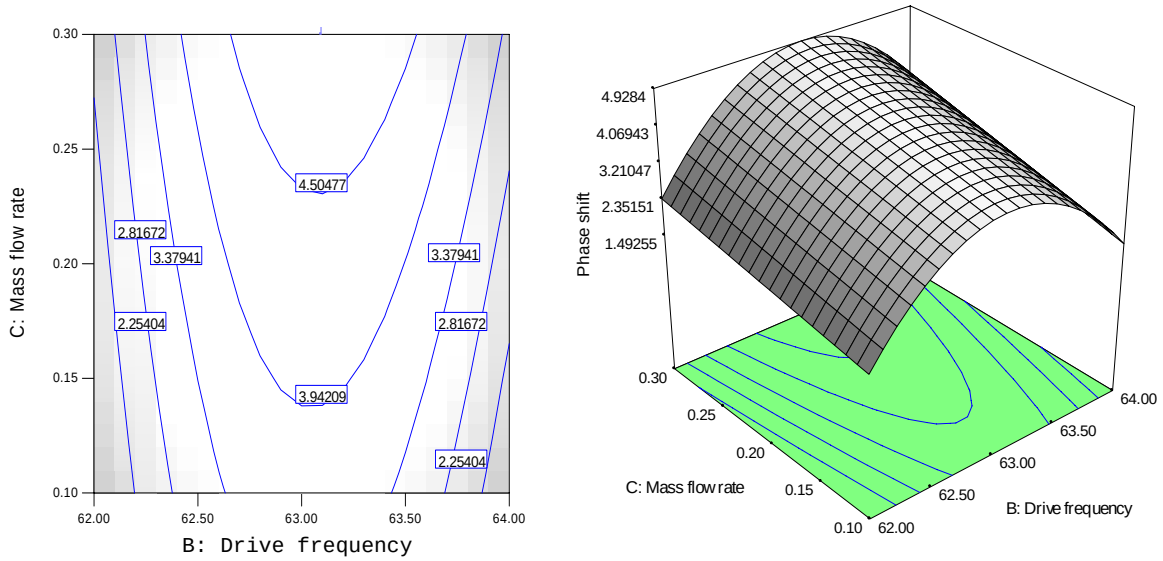

Fig. 7 Response surface predicting phase shift from the model equation: effect of the mass flow rate and the drive frequency at the center level of sensor location

minimum level of mass flow rate but center level of drive frequency.

It is clear from the 3D response surface plots that drive frequency; sensor location and mass flow rate have a significant effect on phase shift. A centre level of sensor location is determined as optimum to achieve maximum phase shift, whereas a maximum level of mass flow rate is determined to achieve maximum phase shift.

7. Conclusions

The application of response surface methodology (RSM) in conjunction with central composite design (CCD) to modeling and optimizing the performance of a Coriolis mass flow sensor was discussed. CCD was used to design an experimental program for modeling the effects of sensor location, drive frequency and mass flow rate on the performance of CMFS. The range of variables of CMFS used in the design were SL 60-120 mm, DF of 62-64 Hz and mass flow rate of 0.1-0.3 kg/s. A total of 20 tests including center points were conducted. A mathematical model equation was derived for phase shift by using the experimental data and the mathematical software package design expert. A predicted value from the model equations was found to be in good agreement with observed values (R^2 value of 0.97 for phase shift). In order to gain a better understanding of the three variables for optimal CMFS performance, the model was presented as 3D response surface graphs. The model allow confident performance prediction by interpolation over the range of data in the database, it was used to construct response surface graphs (Figs. 5-7) to describe the effect of the variables on the performance of a CMFS.

The results show that the all the three variables have a significant effect on phase shift. This study demonstrates that RSM and CCD can be successfully applied to modeling and optimizing CMFS and that it is the economical way of obtaining the maximum amount of information in a short period of time and with the least number of experiments.

Acknowledgement

The authors would like to thank the Department of Science and Technology (DST) Government of India for providing the necessary funding to carry out this research work.

References

1. **Sharma, Satish C.; Patil, Pravin P.; Vasudev, Major Ashish; Jain, S.C.** 2010. Performance evaluation of an indigenously designed copper (U) tube Coriolis mass flow sensors, Measurement 43(9): 1165-1172.
2. **Anklin, Martin: Drahm, Wolfgang; Rieder, Alfred.** 2006. Coriolis mass flowmeters: Overview of the current state of the art and latest research, Flow Measurement and Instrumentation 17: 317-323.
3. **Montgomery, D.C.** 2009. Design and Analysis of Experiments; 7th edition. Hoboken, NJ: Wiley.
4. **Box, G.E.P.; Wilson, K.B.** 1951. On the experimental attainment of optimum conditions, J. R. Stat. Soc. Ser. B 13**:** 1-45.
5. **Myers, R.H.; Khuri, A.I.; Carter, W.H.** 1989. Response surface methodology, 1966-1988 Technometrics 31**:** 137-158.
6. **Myers, R.H.** 1999. Response surface methodology: current status and future directions (with discussion), J. Qual. Technol. 31**:** 30-44.
7. **Rutherford, B. M.; Swiler, L. P.; Paez, T.L.; Urbina, A**. 2006. Response surface (meat-model) methods and applications, Proc. 24th Int. Modal Analysis Conf. (St. Louis, MO): 184-197.
8. **Lee, S.H.; Kwak, B.M.** 2006. Response surface augmented moment method for efficient reliability analysis, Struct. Saf. 28**:** 261-272.
9. **Gavin, H.P.; Yau, S.C.** 2008. High-order limit state functions in the response surface method for structural reliability analysis, Struct. Saf. 30**:** 162-179.
10. **Box, G.E.P.; Hunter**, **W.G.** 1961. The 2k−p fractional factorial designs part I and II, Journal of Technometrics 3: 311-458.
11. **Box, G.E.P.; Hunter, J.S.** 1957. Multi-factor experimental design for exploring response surfaces, Annals of Mathematical Statistics 28: 195-241.
12. Design Expert Software, Version 6, Users Guide, Technical manual, Stat-Ease Inc., Minneapolis, MN, 2004.

Pravin P. Patil, Satish C. Sharma, Roshan Mishra

ALIUMININIO TIPO VAMZDŽIO SVYRAVIMAMS OPTIMIZUOTI NAUDOJAMO ELEKTROMECHANINIO KORIOLIO SRAUTO MASĖS JUTIKLIO CHARAKTERISTIKŲ TYRIMAS TAIKANT PAVIRŠIAUS REAKCIJOS METODOLOGIJĄ

R e z i u m ė

Darbe diskutuojama apie paviršiaus reakcijos metodikos taikymą modeliuojant ir optimizuojant kai kurių projektavimo kintamųjų įtaką Koriolio srauto masės jutiklio charakteristikoms. Trys projektavimo kintamieji: jutiklio padėtis, sužadinimo dažnis ir tekėjimo greitis buvo keičiami atliekant bandymus pagal CCD (Central Composite Design) metodiką. Projekte buvo naudojamos tokios kintamųjų kitimo ribos: jutiklio padėtis 60-120 mm, sužadinimo dažnis 62-64 Hz ir masės tekėjimo greitis 0.1-0.3 kg/s. Naudojant laboratorijoje sukurtą įrangą buvo atlikta 20 bandymų. Masės srauto jutiklio charakteristikoms optimizuoti naudojant kompiuterinę imitavimo programą Expert Dx6, buvo sudarytos matematinio modelio lygtys. Šios lygtys – tai reakcijų antros eilės funkcijos, rodančios fazių poslinkį, priklausomai nuo trijų projektavimo parametrų. Prognozuojami rezultatai gerai sutapo su eksperimentiniais (R^2 vertė fazės poslinkiui yra 0.97). Norint geriau paaiškinti trijų kintamųjų įtaką optimalioms charakteristikoms, buvo parodyti 3D paviršiaus pokyčio modelių paveikslai. Šis tyrimas parodė, kad paviršiaus reakcijos metodologiją ir CCD galima efektyviai naudoti modeliuojant Koriolio srauto masės jutiklio charakteristikas ir tai yra ekonomiškas būdas, per trumpą laiką minimaliu bandymų skaičiumi teikiantis ypač daug informacijos.

Pravin P. Patil, Satish C. Sharma, Roshan Mishra

PERFORMANCE OPTIMIZATION OF ALUMINIUM (U) TYPE VIBRATION BASED ELECTROMECHANICAL CORIOLIS MASS FLOW SENSOR USING RESPONSE SURFACE METHODOLOGY

S u m m a r y

In this study, the application of response surface methodology (RSM) for modelling and optimization of the influence of some design variables on the performance of a Coriolis mass flow sensor is discussed. Three design variables, namely sensor location, drive frequency, and mass flow rate were changed during the experimental tests based on Central composite design (CCD). The range of values of the variables used in the design were a sensor location of 60-120 mm, drive frequency of 62-64 Hz and mass flow rate of 0.1-0.3 kg/s. A total of 20 tests were conducted using the experimental setup developed at laboratory. In order to optimize the performance of mass flow sensor, mathematical model equations were derived by computer simulation programming using design-Expert software (DX6). These equations that are second-order response functions representing phase shift were expressed as functions of three design parameters. Predicted values were found to be in good agreement with experimental values (R^2 values of 0.97 for phase shift). In order to gain a better understanding of the three variables for optimal performance, the models were presented as 3D response surface graphs. This study has shown that the RSM and CCD could efficiently be applied for modeling the performance of Coriolis mass flow sensor and it is an economical way of obtaining the maximum amount of information in a short period of time and with the fewest number of experiments.

Правин П. Патил, Сатиш С. Шарма, Сатиш С. Джейн

ИССЛЕДОВАНИЕ ХАРАКТЕРИСТИК ДАТЧИКА КОРИОЛЯ РАСХОДА МАССЫ С ИСПОЛЬЗОВАНИЕМ МЕТОДОЛОГИИ РЕАКЦИИ ПОВЕРХНОСТИ ПРИМЕНЯЕМОЙ ДЛЯ ОПТИМИЗАЦИИ КОЛЕБАНИИ АЛЮМИНИЕВЫХ ТРУБ ТИПА U

Р е з ю м е

В работе обсуждается влияние некоторых переменных проектирования на характеристики датчика Расхода массы Кориоля при его моделировании и оптимизации применяя методику реакции поверхности. Три переменные: положение датчика, частота возбуждения и скорость потока, изменялись при проведении испытаний по методике CCD (Central Composite Design). В проекте использованы следующие пределы изменения переменных: положение датчика 60-120 мм, частота возбуждения 62-64 Гц и скорость потока массы 0.1-0.3 кг/с. При использовании созданного в лаборатории устройства было проведено 20 испытаний. При оптимизации характеристик датчика расхода массы были составлены уравнения математической модели используя компьютерную программу имитирования Expert Dx6. Эти управления являются функциями второго порядка реакций показывающие сдвиг фаз в зависимости от трех параметров проектирования. Результаты прогнозирования хорошо соответствуют экспериментальным (R^2 значение для сдвига фазы 0.97). Для лучшего пояснения влияния трех перемененных на оптимальные характеристики представлены 3D рисунки моделей изменения поверхности. Это исследование показало, что методологию реакции поверхности и CCD можно эффективно использовать при моделировании характеристик датчика расхода массы Кориоля и это является экономическим способом, обеспечивающим максимальную информацию с минимальной продолжительностью временем и с минимальным числом экспериментов.

Received December 21, 2010
Accepted June 07, 2011